Food Chemistry: Molecular Sciences 5 (2022) 100132

Contents lists available at ScienceDirect

Food Chemistry: Molecular Sciences

journal homepage: www.sciencedirect.com/journal/food-chemistry-molecular-sciences

Multipin cold plasma electric discharge on hydration properties of kodo millet flour: Modelling and optimization using response surface methodology and artificial neural network – Genetic algorithm

Samuel Jaddu, S. Abdullah, Madhuresh Dwivedi, Rama Chandra Pradhan *

Department of Food Process Engineering, National Institute of Technology Rourkela, Odisha 769008, India

ARTICLE INFO

Keywords:
Thermograph
Voltage
Time
Treatment
Functional properties

ABSTRACT

The effect on functional properties of kodo millet flour was studied using multipin cold plasma electric reactor. The analysis was carried out at various levels of voltage (10–20 kV) and treatment time (10–30 min) for four different parameters such as water absorption capacity (WAC), oil absorption capacity (OAC), solubility index (SI) and swelling capacity (SC). Response surface methodology (RSM) and artificial neural network – genetic algorithm (ANN – GA) were adopted for modelling and optimization of process variables. The optimized values obtained from RSM were 20 kV and 17.9 min. On the contrary, 17.5 kV and 23.3 min were the optimized values obtained from ANN – GA. The RSM optimal values of WAC, OAC, SI and SC were 1.51 g/g, 1.40 g/g, 0.06 g/g and 3.68 g/g whereas optimized ANN – GA values were 1.51 g/g, 1.50 g/g, 0.06 g/g and 4.39 g/g, respectively. Infrared spectra, peak temperature, diffractograms and micrographs of both optimized values were analyzed and showed significant differences. ANN showed a higher value of R^2 and lesser values of other statistical parameters compared to RSM. Therefore, ANN – GA was treated as the best model for optimization and modelling of cold plasma treated kodo millet flour. Hence, the ANN – GA optimized values of cold plasma treated flour could be utilized for practical applications in food processing industries.

1. Introduction

Millets are extensively cultivated in Asian and African countries. India, one of the significant millet producing countries, cultivates various types of millets, generally categorized as 'coarse grain cereals' (Hegde, Chandrakasan, & Chandra, 2002). Among different millets produced in India, kodo, little, barnyard, proso and foxtail millet etc., are termed as 'minor millets' due to their under utility. The kodo millet (*Seritia italica*), with high antioxidant activity and significant anti-diabetic capacity, is one of the most critical minor millet primarily produced in the subcontinents of India (Arya & Shakya, 2021; Sharma, Saxena, & Riar, 2017). Kodo millet contains higher amounts of crude fibre (14.3 g) and total phenolic content (10.3 mg) as compared to other millets (Rao, Nagasampige, & Ravikiran, 2011). In addition, kodo millet does not form a gluten network and could be an alternative for those suffering with celiac disease or various intolerances/allergies of wheat. Furthermore, it is very much beneficial to people who have diabetes since the kodo millet contains complex carbohydrates that allow the slowest release of glucose into the blood, which minimises the glycaemic index. Hence, along with a high nutritional profile of the kodo millet with carbohydrates 66.1 g, protein 8.3 g, ash 2.6 g, fat 1.4 g, and energy value 355 kcal adds nutritional security to the vast population (Nanje Gowda et al., 2022).

However, a significant share of the total kodo millet produced in the country is directly consumed by the rural population. Because of this, the actual value of millets has not been appropriately studied, and their utilization has been not appreciated so far in view of food security (Sharma, Sharma, Handa, & Pathania, 2017). Considering the potential health benefits such as anti-carcinogenic anti-oestrogenic, anti-inflammatory, and antiviral effects (Ferguson, 2001) and no gluten content in kodo millet, it is commonly used to make bakery products like bread, biscuit, etc (Sharma, Saxena, & Riar, 2016).

The improvement in the millet flour functional properties is essential to enhance the desired qualities of the final products. Nevertheless, there is a challenge involved in attaining the preferred increase in the functional properties of flour without adversely affecting its heat labile nutrients. Different treatments were employed for enhancing the flour hydration and gel properties in various millet and cereal flours like

* Corresponding author.
E-mail addresses: dwivedim@nitrkl.ac.in (M. Dwivedi), pradhanrc@nitrkl.ac.in (R.C. Pradhan).

https://doi.org/10.1016/j.fochms.2022.100132
Received 17 June 2022; Received in revised form 18 August 2022; Accepted 29 August 2022
Available online 5 September 2022

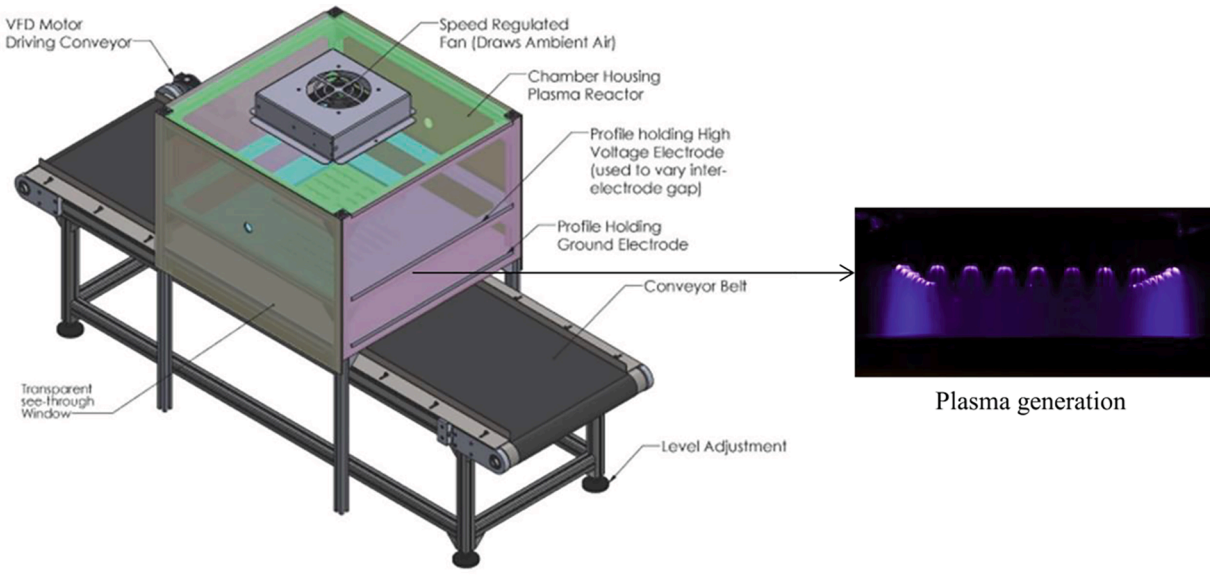

Fig. 1. Schematic diagram of multipin cold plasma reactor (adapted from M/s. Ingenium Naturae pvt. ltd., Gujarat, India).

germination, pre-gelatinization, microwave cooking, etc. Previous studies stated that functional properties of whole corn was improved by extrusion and germination methods. Cassava flour along with other flours such as popped rice and wheat flours, rice and wheat brans made as collective flour and their functional properties positively modified through pre-gelatinization treatment and pre-treatment with amylase enzyme (Jisha, Padmaja, Moorthy, & Rajeshkumar, 2008). The hydration properties of foxtail millet by microwave treatment resulted in more SI and WAC whereas SC and OAC were reduced. The microwave treatment of proso and little millet flour were increased their functional properties (Rao et al., 2021). By use of either thermal treatment or imbibition, the functional properties of cereal and millet flours were increased. These treatments have disadvantages like reduction of heat sensitive components in thermal processing and needs long time for enhancing the functional properties in germination. Novel technologies could be alternative for attaining the improvement in functional properties without prolonging time and no heat treatment.

Cold plasma can be a promising method to improve the functional properties of millet and cereal flours. During generation of plasma, many reaction species are released particularly reactive nitrogen and oxygen species and their action on flour enhances functional properties by dissociation of starch granules (Jaddu, Pradhan, & Dwivedi, 2022). Hence, cold plasma technology was adopted to achieve the desired characteristics of kodo millet flour. RSM and ANN – GA were used for

Table 1a
Experimental and predicted responses of RSM and ANN models.

Run	Voltage	time	WAC			OAC			SI			SC		
			Expt	RSM Predd	ANN Predd	Expt	RSM Predd	ANN Predd	Expt	RSM Predd	ANN Predd	Expt	RSM Predd	ANN Predd
1	15	20	1.49 ± 0.05	1.48	1.48	1.40 ± 0.09	1.40	1.40	0.076 ± 0.01	0.071	0.074	3.67 ± 0.55	3.77	3.75
2	7.9	20	1.56 ± 0.04	1.56	1.56	1.31 ± 0.07	1.31	1.30	0.095 ± 0.03	0.092	0.095	3.94 ± 0.39	3.94	3.94
3	15	20	1.50 ± 0.05	1.48	1.48	1.38 ± 0.09	1.40	1.40	0.061 ± 0.03	0.071	0.074	3.67 ± 0.55	3.77	3.75
4	15.0	34.1	1.50 ± 0.05	1.49	1.50	1.41 ± 0.07	1.42	1.41	0.108 ± 0.03	0.107	0.111	3.65 ± 0.19	3.68	3.65
5	15.0	20	1.48 ± 0.07	1.48	1.48	1.41 ± 0.04	1.40	1.40	0.072 ± 0.03	0.071	0.074	3.83 ± 0.48	3.77	3.75
6	20	30.0	1.49 ± 0.03	1.49	1.49	1.43 ± 0.03	1.42	1.43	0.076 ± 0.01	0.076	0.076	3.74 ± 0.23	3.73	3.65
7	10	30.0	1.53 ± 0.02	1.54	1.53	1.37 ± 0.06	1.36	1.37	0.109 ± 0.00	0.111	0.109	3.92 ± 0.23	3.89	3.93
8	15	20	1.47 ± 0.07	1.48	1.48	1.41 ± 0.04	1.40	1.40	0.066 ± 0.03	0.071	0.074	3.83 ± 0.48	3.77	3.75
9	10	10	1.55 ± 0.05	1.54	1.56	1.33 ± 0.03	1.33	1.33	0.075 ± 0.01	0.079	0.081	3.47 ± 0.45	3.52	3.47
10	22.1	20	1.53 ± 0.16	1.53	1.52	1.39 ± 0.04	1.39	1.39	0.057 ± 0.01	0.056	0.057	3.76 ± 0.28	3.72	3.76
11	15	5.9	1.52 ± 0.04	1.53	1.52	1.37 ± 0.09	1.38	1.36	0.080 ± 0.02	0.076	0.080	3.26 ± 0.14	3.18	3.09
12	20	10	1.55 ± 0.03	1.54	1.55	1.39 ± 0.11	1.39	1.38	0.062 ± 0.02	0.065	0.062	3.31 ± 0.15	3.38	3.17
13	15	20	1.47 ± 0.07	1.48	1.48	1.41 ± 0.04	1.40	1.40	0.078 ± 0.01	0.071	0.074	3.83 ± 0.48	3.77	3.75

WAC – Water absorption capacity; OAC – Oil absorption capacity; SC – Swelling capacity; SI – Solubility index; Expt – experimental; RSM Predd – RSM predicted; ANN Predd – ANN predicted; all the parameters were expressed in g/g.

modelling and optimization of process variables of kodo millet flour. Two methodologies namely RSM and ANN models have been applied simultaneously in many studies for a clear interpretation of the process by previous studies (Pradhan et al., 2021). Hence, both RSM and ANN models are used to obtain best combination for commercial application of treated flour. However, the effect of cold plasma studies on the functional properties of millets is scarce. And also, studies have not been reported on applying ANN – GA to model and optimize the functional properties of kodo millet using cold plasma. Hence, the objectives of this study are: (a) to determine the effect of process parameters (treatment time and plasma voltage) using multipin cold plasma electrical discharge on the functional properties of kodo millet flour; b) to optimize the process parameters of the multipin cold plasma treatment on kodo millet flour to obtain the desired functional properties; (c) to compare and evaluate the performance of models of RSM and ANN – GA used to optimize the plasma-treated kodo millet flour.

2. Materials and methods

Kodo millet was purchased from the Indian Institute of Millet Research, Hyderabad, Telanagana, India. Kodo was initially dried, cleaned and dehulled. Dehulled millet was milled in an impact (hammer) mill to obtain flour (Indosaw Products Pvt. ltd., Ambala, Haryana, India) and passed through ASTM mesh no 70 to get fine particle sizes (Cordelino et al., 2019). Grinded flour was sealed in zip lock covers and stored for analysis.

2.1. Plasma experimental set up

Multipin cold plasma reactor (Ingenium Naturae Private Limited, Gujarat, India, IN-HVLT MP) was used for conducting experiments with the following specifications: Current 5 mA, input voltage 230 V, and frequency 50 Hz, and fixed and output voltage maximum of 60 kV. The cold plasma reactor with top view is drawn in Fig. 1. The reactor consists of discharging area having 1.85 × 2.50 cm^2 and high voltage upper electrode consists of total 63 pins. Both electrodes in plasma reactor made with stainless steel for ensuring long life. Generation of plasma occurs with combination of ambient air and normal atmospheric pressure. 1–2 mm layer of millet flour was kept in sample pan under plasma reactor. Constant distance (3 cm) was placed in both the electrodes for all the treatments. Voltage below 10 kV and treatment times of below 10 min and above 30 min for both output voltages did not show any significant change during preliminary studies on hydration properties. As distance kept constant at 3 cm, maximum voltage obtained with constant distance was 20 kV. Henceforth, flour was treated at two output voltages 10 kV and 20 kV.

2.2. Experimental design

A Box behnken factorial design from the design expert software (Version 11.0.5.0, Start-Ease Inc.) was used to get the combination of independent variables and the number of experimental runs. A total of 17 experiments were conducted according to the experimental design shown in Table 1a. All the experiments were conducted in triplicate and each experiment was carried out using 15 g of kodo millet flour.

2.3. Modelling and optimization

2.3.1. Response surface methodology (RSM)

Modelling and optimizing the various combinations of process variables to acquire maximum values of dependent variables, RSM was used. In order to predict the optimized values for independent variables, 2nd order polynomial regression model was used to analyse the experimental data. The equation was given as follows.

$$Y = b_o + \sum_{l=1}^{k} b_e x_l + \sum_{m=1}^{k} b_{ff} x_m^2 + \sum \sum_{e<f} b_{ef} x_l x_m \quad (1)$$

The graphical analysis, regression analysis, and experimental design were developed in Design Expert software (version 10.0.3.0., Stat-Ease Inc.).

where Y is the response predicted values, x_l and x_m are the real values of independent variables and b_o, b_{ff}, b_{ef}, and b_e are the regression coefficients for quadratic, interaction, and linear, terms, respectively, and. Statistical analysis, validation of developed regression model, significance of regression coefficients in the equation, and significance of the independent variables effect were evaluated using analysis of variance (ANOVA).

2.3.2. Artificial neural network – Genetic algorithm (ANN – GA)

MATLAB fitting of neural network and toolboxes contains genetic algorithm (The Math Works, Inc., Natick, MA, version R2015a) were used for modelling and optimization of responses, combined ANN – GA. ANN consists of input layer, hidden layer, and output layer for every dependent response were determined. Two number of neurons was considered in the input layer such as voltage (A) and time (B). The hidden layer neurons were obtained by trial and error method at 12 neurons to get the maximum R^2 and minimum MSE values. The training for each and every response such as WAC (R_1), OAC (R_2), SI (R_3) and SC (R_4) were conducted separately, and hence, the only one neuron output layer was achieved.

The output and input data sets are translated to coded form for easy handling and convenience before proceeding for ANN training. The codes used for input data were in between −1 and +1. Similarly for output data were in between 0 and +1. The cold plasma treatment process for kodo millet flour was designed using box behnken with two input parameters. Hence, four different training were performed for every response. Each training was performed for 13 data set of three neurons with only one output neuron and all the data sets were designated in to training, testing and validation for every response. Linear function (*purelin*) in output layer and hyperbolic sigmoid (*tansig*) in hidden layer was used as transfer functions. Levenberg–Marquardt back propagation (*trainlm*) algorithm was used for 58.33 % training, 25 % validation and 25 % testing of total data.

To obtain high maximum R^2 and low MSE, network is trained accordingly. After training, Equation (2) was used for generating the weights and bias values and there after predicting the values of the responses (Xj) with the developed model.

$$Y_j = purelin\ [W_{OH} \times \text{tansig}\ (U_{IH} \times X_j + TH) + TO] \quad (2)$$

where Xj, Yj are the experimental input and predicted output responses. The U_{IH} and W_{OH} are the weights between the input and hidden layers and the hidden and output layers, respectively. The TH and TO are the bias values of the hidden and output layer neurons, respectively.

Further, GA was employed to developed model to optimize the input parameters. The fitness function (f) was adopted to optimize all the dependent parameters for maximizing values using the Equation (3) (Pradhan, Abdullah, & Pradhan, 2020).

GA was selected as the population type with double vector, creation function with feasible population, fitness scaling function with rank, selection function with roulette wheel function, crossover function with scattered, migration with forward migration, and mutation function with adaptive feasibility respectively.

Moreover, the size of the population was selected as 200 because of the repetition of GA loop, and less than 200 iterations were came. The crossover fraction was selected as 0.8 and the remaining functions were set as by default for the achieving best optimization result. All selected parameters were based on their properties reported by previous researchers (Abdullah, Pradhan, Aflah, & Mishra, 2020; Patra, Abdullah, & Pradhan, 2021; Pradhan et al., 2021). The fitness function (f), which

Table 1b
Second order polynomial equations of treated kodo millet flour.

Coefficients	WAC			OAC			SI			SC	
	RSM	ANN		RSM	ANN		RSM	ANN		RSM	ANN
A	−0.01004			0.029264			−0.01246			−0.07686	
B	−0.01275			0.015682			0.010927			0.178311	
AB	−0.01086			0.000377			−0.00518			−0.00404	
A^2	0.032251			−0.0249			0.001587			0.031024	
B^2	0.014542			−0.00293			0.010562			−0.16762	
R-Square	0.9202	0.9306	R-Square	0.9214	0.9307	R-Square	0.9197	0.9226	R-Square	0.9087	0.9220
Adj R-Square	0.8633		Adj R-Square	0.8653		Adj R-Square	0.8623		Adj R-Square	0.8434	
Pred R-Square	0.6775		Pred R-Square	0.6741		Pred R-Square	0.7674		Pred R-Square	0.6831	
R VALUE	**0.9593**	**0.9647**	R VALUE	**0.9599**	**0.9647**	R VALUE	**0.959**	**0.9605**	R VALUE	**0.9532**	**0.9602**

was used in the ANN – GA optimization process, is given below.

$$f = -(P_1 + P_2 + P_3 + P_4) \quad (3)$$

where, P_1, P_2, P_3 and P_4 are the ANN – GA predicted responses WAC, OAC, SI and SC, respectively, and the negative sign indicates the maximization of the given function in the GA.

2.4. Functional properties

2.4.1. Water and oil absorption capacity:

1 g of millet flour was measured for both WAC and OAC. 10 ml of (water/oil) was added to flour and kept for 30 min resting. The contents were centrifuged at 3000 g for 15 min. the weight of water and oil absorbed by flour was recorded. The water and oil absorption capacity was determined and calculated by using Equations (4 & 5) mentioned in previous study. (Ramashia, Gwata, Meddows-Taylor, Anyasi, & Jideani, 2018).

$$WAC = \frac{B}{A} \quad (4)$$

$$OAC = \frac{C}{A} \quad (5)$$

Where A = Sample weight (g).
B = Weight of flour absorbed by water (g).
C = Weight of flour absorbed by oil (g).

2.4.2. Solubility index and swelling capacity:

Millet flour (0.5 g – SI, 0.1 g – SC) was weighed and mix with 10 ml of distilled water. The contents were kept in water bath at 60 °C for 0.5 h. The solution was centrifuged at 1600 g for 10 min. The supernatant of 5 ml quantity was dried and measured. For SC, the contents were kept at 60oC with continuous shaking for 0.5 h. After centrifuge at 1600 g for 15 min, the water bound to flour was measured. Solubility index and swelling capacity was estimated and calculated by using Equations (6 & 7) reported in previous study. (Kusumayanti, Handayani, & Santosa, 2015).

$$SI = \frac{E}{D} \times 2 \quad (6)$$

$$SC = \frac{F}{D} \quad (7)$$

Where D = Sample weight in dry basis (g).
E = Soluble starch weight (g).
F = Precipitate weight (g).

2.4.3. Differential scanning calorimeter (DSC)

Differential scanning calorimeter (NETZSC; Maia 200F3, USA) was used to measure the gelatinization temperature of kodo millet flour with plasma treatment. 10–15 mg of flour was placed in Aluminium sample holder (pan and lid) and nitrogen used as a purge gas. The temperature range used to find out the peak temperatures at 30 to 150 °C with 10 °C /min heating rate.

2.4.4. Fourier transform Infrared spectrometry (FTIR)

FTIR spectrometry (Bruker, Alpha E FTIR, Germany) with attenuated total reflectance (ATR) was used for measuring infrared spectra for treated KMF. Before taking every measurement, the background has to be set. Wavenumbers ranged from 500 to 4000 cm^{-1} with 32 scans per each sample was used to measure the transmittance (%) in spectra.

2.4.5. X-ray diffraction (XRD) analysis

X-Ray diffractometer (AXS D8 Advance with Davinci Design, Bruker, Germany) used to analyze the diffractograms of treated KMF with 40 mA, 40 kV and 2θ angle (5–50°), 4°/min scanning rate and 0.02 step size.

2.4.6. Scanning electron microscopy (SEM)

The micrographs of plasma treated KMF was observed in scanning electron microscopy (JEOL JSM- 6480 LV, EDS: Oxford Instruments, Japan) at 5 μm particle size, 5000x magnification, accelerated voltage 15 kV.

2.5. Statistical analysis

Various statistical parameters of developed models from RSM and ANN – GA were compared. The parameters such as average mean square error (MSE), root mean square error (RSME), normal mean square error (NMSE), normal root mean square (NRMSE), absolute deviation (AAD), mean percentage error (MPE), and coefficient of determination (R^2) using the formulas given in the Equation (8–14). The model with less MSE, RSME, NSME, NRSME, AAD, and higher R^2 was selected as the best model for the response expression.

$$MSE = \frac{\sum (X_P - X_a)^2}{n} \quad (8)$$

$$RMSE = \sqrt{\frac{\sum (X_P - X_a)^2}{n}} \quad (9)$$

$$NMSE = \frac{MSE}{X_m} \quad (10)$$

$$NRMSE = \frac{RMSE}{X_m} \quad (11)$$

$$AAD = \frac{\sum |X_P - X_a|}{n} \quad (12)$$

$$MPE = \frac{100}{n} \sum \left| \frac{(X_P - X_a)}{Xp} \right| \quad (13)$$

$$R^2 = 1 - \frac{\sum (X_P - X_a)^2}{\sum (X_P - X_m)^2} \quad (14)$$

Table 2a
Training, testing and validation of ANN Model.

WAC			OAC			SI			SC		
Training	Testing	Validation	Training	Testing	Validation	Training	Testing	Validation	Training	Testing	Validation
2	1	5	3	1	2	1	2	3	1	3	6
4	3	10	4	6	5	5	9	4	2	11	8
6	9	13	7	12	11	6	13	8	4	12	13
7			8			7			5		
8			9			10			7		
11			10			11			9		
12			13			12			10		

3. Results and discussion

Two models such as response surface methodology and artificial neural network were used for modeling and numerical optimization and genetic algorithm for optimization of treated kodo millet flour.

3.1. Response surface methodology

3.1.1. Fitting of RSM model

Two parameters (independent) such as voltage, and treatment time and their effect on the four dependent variables (WAC, OAC, SI and SC) for cold plasma treated kodo millet flour were tabulated in Table 1a. Second order polynomial equations of R^2, adj R^2 and pred R^2 for kodo millet flour after treatment were presented in Table 1b. The results from ANOVA of all four dependent parameters for the developed model indicated the models are acceptable with required R^2, pred R^2, and adj R^2. R^2 value higher than 0.8 for a generated regression model is desirable as reported by previous studies (Sin, Yusof, Hamid, & Rahman, 2006). Moreover, necessary statistical parameters such as MSE, RSME, AAD, and MPE of the desirable model must be minimum (Abdullah et al., 2020). The models developed models for all variables (dependent) have an R^2 greater than 0.9 with minimum MSE, RSME, AAD, and MPE. All the dependent variables showed that lack fit were not significant. Besides, all the dependent parameters have an insignificant lack of fit. These results show that the developed model indicated that was well fitted.

3.1.2. Cold plasma effect on water absorption capacity

From Equation (15), process variables such as voltage (A) and time (B) at $p < 0.05$, had a significant negative effect on the WAC. The interaction term AB had a negative effect and does not show any significant effect, and both the quadratic terms A^2 and B^2 ($p < 0.001$; $p < 0.05$) showed a significant increase in WAC. From supplementary (sup.) Fig. 1a, the WAC decreased with time 20 min and after 20 min significant rise in WAC. On the other side, WAC with voltage also decreased upto15 kV and subsequent increase after 15 kV. Similar studies reported that rise in WAC of kodo millet flour might due to abundance of various hydrophilic compounds in flour particularly, carbohydrates, proteins, and more over residues of polar amino acids showed higher attraction to H_2O molecules (Godswill, Somtochukwu, & Kate, 2019).

$$WAC = 1.480673 - 0.01004A - 0.01275B - 0.01086AB + 0.032251A^2 + 0.014542B^2 \quad (15)$$

3.1.3. Cold plasma effect on oil absorption capacity

From Equation (16), process variables such as voltage (A) and time (B) ($p < 0.001$; $p < 0.01$), had a significant increase in OAC. Likewise, the interaction term AB had no significant effect (positive) up on OAC. On contrary, the quadratic terms A^2 ($p < 0.01$) showed a significant negative impact on OAC and B^2 does not show any significant effect (negative correlation) on OAC. From sup. Fig. 1b, it was showed that the significant rise in OAC while increasing time. Similar manner increased OAC observed at voltage upto16 kV, thereafter gradual reduction in OAC above 16 kV. The non-polar amino acids and other structures of protein present in flour may lead to increase in OHC. Previous works reported that the presence of non-polar amino acids, protein content and the bulk density of the protein powder influence the OHC of wheat flour. There was no significant change in OHC may be due to modifications in the flour protein structures of wheat grain and with plasma treatment (Chaple et al., 2020).

$$OAC = 1.406309 + 0.029264A + 0.015682B + 0.000377AB - 0.0249A^2 - 0.00293B^2 \quad (16)$$

3.1.4. Cold plasma effect on solubility index

From Equation (17), process variables such as voltage (A) ($p < 0.05$), had observed reduction in SI and time (B) ($p < 0.05$), had a positive effect on the estimation of SI. The interaction term AB had a negative correlation on SI. However, the quadratic terms A^2 showed a positive impact on SI and B^2 ($p \leq 0.01$) had a significant positive effect on SI. From sup. Fig. 1c, the significant rise of SI along with increase time and voltage up to 16 kV. SI was gradually decreased when voltage exceeds 16 kV. The oxidation of starch and molecular degradation caused by active species of plasma especially ROS and RNS thus made the more solubility was reported in earlier studies (Bie et al., 2016).

$$SI = 0.07068 - 0.01246A + 0.010927B - 0.0518AB + 0.001587A^2 + 0.010562B^2 \quad (17)$$

3.1.5. Cold plasma effect on swelling capacity

From Equation (18), process variables such as voltage (A) ($p < 0.05$) had shown a negative correlation against SC and on contrary, time (B) ($p < 0.001$), had a positive effect on the SC significantly. On other hand, the interaction term AB had no significant effect (negative correlation) on it. The quadratic term A^2 did not have significant positive impact on SC but quadratic term B^2 ($p \leq 0.01$) showed a significant decreased effect on SC. Sup. Fig. 1d, observed that the gradual increase of SC lead to significant effect with increase in time. Beyond 16 kV voltage, there was a decreased trend observed in SC. The starch granules became weak due to presence of binding forces resulted in increased swelling power (Obadi et al., 2018).

$$SC = 3.765821 - 0.07686A + 0.178311B - 0.00404AB + 0.031024A^2 - 0.16762B^2 \quad (18)$$

3.2. Artificial neural network – genetic algorithm

3.2.1. Model fitting

The experimental data (with 12 data points) obtained using Box–Behnken design was initially divided randomly into 3 sets: 7, 3, and 3 (approximately 58.33 %, 25 %, and 25 % of data sets) for training, validation, and testing, respectively. Training determines the network

parameters, validation indicates the robustness of the network parameters, and testing controls the error in the network parameters (Patra et al., 2021; Abdullah, Pradhan, Pradhan, & Mishra, 2021). From Table 2a, WAC runs 2, 4, 6, 7, 8, 11 and 12 were used for training, runs 5, 10 and 13 were used for validation and finally runs 1, 3 and 9 were used for testing. The weights and bias values obtained after training were given for water absorption capacity in Eqs. (19)–(22), which were used to predict the output data. Error histogram and post-training performance of water absorption capacity of generated artificial neural network model was given in sup. Fig. 2a.

$$UA = \begin{bmatrix} 1.59471 & -4.44029 \\ -4.84890.005576 & \\ 2.53206 & -4.13018 \\ 1.871821 & -4.46699 \\ -4.85074 & -0.11595 \\ 3.682589 & -3.16175 \\ 2.834384 & -3.92426 \\ -4.404791.996104 & \\ -0.34296 & -4.85978 \\ 4.2812512.447735 & \\ -1.58407 & -4.55396 \\ 2.017433 & -4.67318 \end{bmatrix} \quad (19)$$

$$THA = \begin{bmatrix} 4.993654 \\ 3.969162 \\ -3.0916 \\ -2.1938 \\ 1.336898 \\ -0.68783 \\ 0.167625 \\ -1.3199 \\ -2.17124 \\ 2.966334 \\ -4.00195 \\ 4.587474 \end{bmatrix} \quad (20)$$

$$WA = [0.905217\ 0.166432\ 0.060521\ -0.38616\ -0.3217\ 0.546673\ 0.039283\ 0.364819\ 0.48904\ -0.73252\ -0.41739\ -0.59743] \quad (21)$$

$$TOA = [0.09983] \quad (22)$$

OAC runs 3, 4, 7, 8, 2, 5 and 11 were used for training, runs 1, 6 and 12 were used for validation and finally runs 5, 9 and 12 were used for testing. The weights and bias values obtained after training were given for oil absorption capacity in Eqs. (23)–(26), which were used to predict the output data. Error histogram and post-training performance of oil absorption capacity of generated artificial neural network model was given in sup. Fig. 2b.

$$UB = \begin{bmatrix} -2.13118 & -4.34041 \\ 4.653071.413812 & \\ 4.8452580.360692 & \\ 4.0860962.525124 & \\ 4.8492590.008394 & \\ -3.15309 & -3.70224 \\ 4.8450680.227237 & \\ -3.804243.018254 & \\ 4.804971 & -0.67474 \\ 2.795647 & -3.96789 \\ -4.166692.54633 & \\ 2.333004 & -4.33386 \end{bmatrix} \quad (23)$$

$$THB = \begin{bmatrix} 4.865711 \\ -3.95331 \\ -3.07667 \\ -2.27938 \\ -1.31674 \\ 0.073726 \\ 0.435896 \\ -1.30943 \\ 2.18748 \\ 3.076782 \\ -3.93724 \\ 4.777131 \end{bmatrix} \quad (24)$$

$$WB = [-0.06877\ -0.49605\ -1.06262\ 0.451493\ 0.593644\ -0.76347\ -0.28245\ -0.37569\ 0.425664\ 0.446138\ 0.505143\ -0.4295] \quad (25)$$

$$TOB = [-0.10799] \quad (26)$$

SI runs 1, 5, 6, 7, 10, 11 and 12 were used for training, runs 3, 4 and 8 were used for validation and finally runs 2, 9 and 13 were used for testing. The weights and bias values obtained after training were given for solubility index in Eqs. (27)–(30), which were used to predict the output data. Error histogram and post-training performance of solubility index of generated artificial neural network model was given in sup. Fig. 2c.

$$UC = \begin{bmatrix} -4.17532.253175 & \\ 2.3288124.334823 & \\ -2.34567 & -4.26125 \\ 4.1212072.531036 & \\ -3.18619 & -3.64544 \\ 2.084526 & -4.42852 \\ -1.138194.740746 & \\ 3.3775933.470586 & \\ -4.67133 & -0.23947 \\ 4.549718 & -1.68199 \\ -3.88674 & -2.96263 \\ -4.00227 & -2.67739 \end{bmatrix} \quad (27)$$

$$THC = \begin{bmatrix} 4.969055 \\ -3.88971 \\ 3.113399 \\ -2.229 \\ 1.432547 \\ -0.6638 \\ 0.096963 \\ 1.334031 \\ -2.44626 \\ 3.084328 \\ -3.85758 \\ -4.88269 \end{bmatrix} \quad (28)$$

$$WC = [0.248546\ -0.54324\ 1.048601\ 0.331394\ -0.70007\ -0.77222\ 0.335066\ 0.234839\ 0.096795\ 0.142094\ 0.566386\ -0.05296] \quad (29)$$

$$TOC = [-0.66005] \quad (30)$$

SC runs 1, 2, 4, 5, 7, 9 and 10 were used for training, runs 6, 8 and 13 were used for validation and finally runs 3, 11 and 12 were used for testing. The weights and bias values obtained after training were given for swelling capacity in Eqs. (31)–(34), which were used to predict the

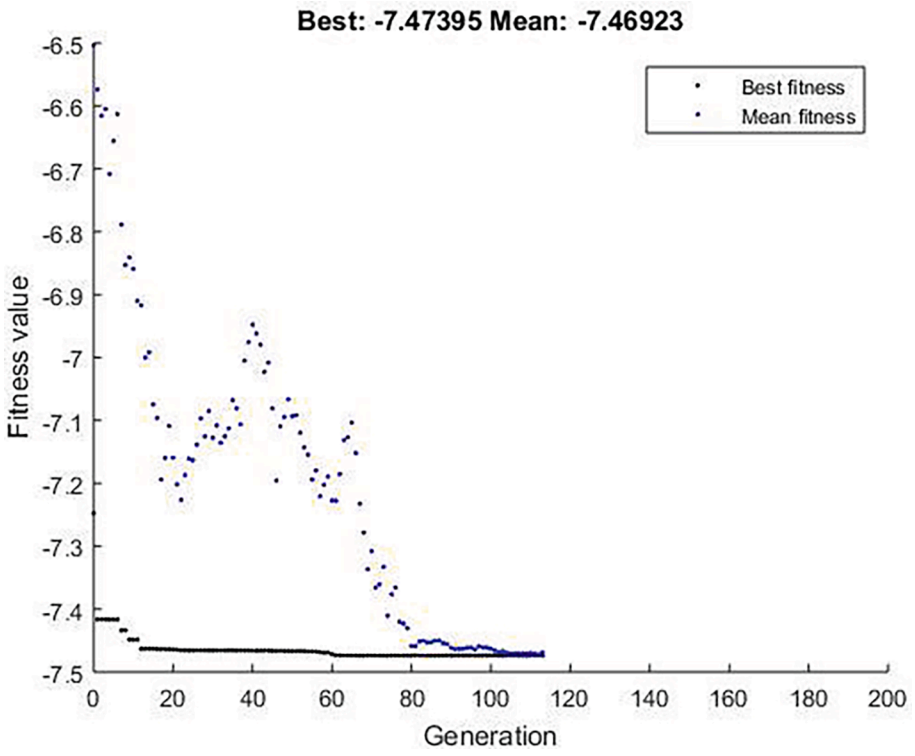

Fig. 2. The fitness variation in terms of generations during optimization of genetic algorithm.

output data. Error histogram and post-training performance of swelling capacity of generated artificial neural network model was given in sup. Fig. 2d.

$$UD = \begin{bmatrix} -3.75535 - 3.14433 \\ 3.840377 - 3.05022 \\ 0.488754 - 4.82231 \\ 4.856106 - 0.14392 \\ 4.826028 - 0.47633 \\ -2.56504 - 4.11781 \\ 2.9770023.836292 \\ 4.7728480.869371 \\ -1.276624.712935 \\ -4.51758 - 1.7569 \\ 3.5824633.269056 \\ -4.56032 - 1.65096 \end{bmatrix} \quad (31)$$

$$THD = \begin{bmatrix} 4.777303 \\ -3.89537 \\ -3.08804 \\ -2.19692 \\ -1.29212 \\ 0.44191 \\ 0.361868 \\ 1.2831 \\ -2.14135 \\ -3.08975 \\ 3.967796 \\ -4.84933 \end{bmatrix} \quad (32)$$

$$WD = [0.510167 \ -0.12319 - 0.27937 \ 0.362828 \ -0.46989 \ -0.21889 \ -0.83235 \ 0.080834 \ 0.835196 \ -0.44547 - 0.06046 \ 0.699726] \quad (33)$$

$$TOD = [0.13094] \quad (34)$$

A neural network model consists of a single input, and hidden and output layers. It is necessary to finalize the number of neurons in the hidden layer to build the best ANN model for the prediction of the responses. This was confirmed by repeatedly training the network until minimum MSE and maximum R was achieved. After repeated training, the number of neurons in the hidden layer was selected as 12, since it had a minimum MSE of 0.000071, 0.000087, 0.000021, and 0.003929 and maximum R of 0.9647, 0.9647, 0.9605, and 0.9602 for training, testing, validation, and all data sets, respectively.

3.3. Optimization

After modeling of both RSM and ANN – GA, these models were optimized.

3.3.1. Numerical optimization

The combination with maximum desirability was selected as the optimum condition for the cold plasma treatment of millet flour. The selected optimum condition was voltage of 20 kV and treatment time of 17.1 min. The WAC, OAC, SI and SC of treated kodo millet flour at this recommended optimum combination were 1.50845 g/g, 1.40447 g/g, 0.05907 g/g and 3.67574 g/g, respectively.

3.3.2. GA optimization

To improve functional properties like WAC, OAC, SI, SC, independent variables (voltage and treatment time) were optimized by GA. The optimization was carried out using individual and mean fitness values to attain MSE and RSME. The optimization cycle was extended even after mutation and if the desired output was not reached, then whole population was repeated for production, mutation and crossover for the next generation. The graph between the number of generations and the fitness value was shown in Fig. 2. The figure shows till 12th generation, no change in the fitness value, and the mean fitness value calculated as −7.47395. The optimization was successful at conditions of 17.1 kV voltage and 23.3 min treatment time. At these optimized conditions, the predicted values of WAC, OAC, SI and SC were obtained as 1.5129 g/g, 1.5002 g/g, 0.0616 g/g and 4.388 g/g, respectively.

Both the numerical and GA optimization was validated by conducting experiments at the obtained optimum conditions and verifying

Table 2b
Summary of all statistical parameters (AAD, MSE, RSME, NMSE, NRSME, MPE and R^2) of variable parameters.

Coefficient	WAC		OAC		SI		SC	
	RSM	ANN	RSM	ANN	RSM	ANN	RSM	ANN
AAD	0.00783	0.00657	0.00815	0.00875	0.00397	0.00326	0.06034	0.06943
MSE	0.00008	0.00007	0.00009	0.00010	0.00002	0.00003	0.00431	0.00747
RMSE	0.00877	0.00853	0.00969	0.01009	0.00473	0.00507	0.06566	0.08644
NMSE	0.00005	0.00005	0.00007	0.00007	0.00029	0.00033	0.00117	0.00203
NRMSE	0.00581	0.00565	0.00699	0.00728	0.06056	0.06485	0.01783	0.02348
MPE	0.52101	0.43743	0.58309	0.63055	5.35311	4.24018	1.66096	1.99149
R^2	0.92023	0.93060	0.92143	0.93074	0.91965	0.92263	0.90867	0.92204

All the parameters were expressed in g/g.

no significant difference between the predicted and experimental responses.

3.3.3. *Comparing optimized results*

The models developed from both RSM and ANN and their predicted values were compared statistically using different parameters such as AAD, R^2, MSE, NSME, RSME, NRSME, and MPE, and all were presented in Table 2b. Both the models have showed better predictability for all the statistical parameters. However, ANN model indicated higher R^2 values than RSM upon comparison. And remaining parameters such as AAD, MSE, NSME, RSME, NRSME, and MPE are minimum values for the ANN model than RSM model. These obtained results revealed that ANN

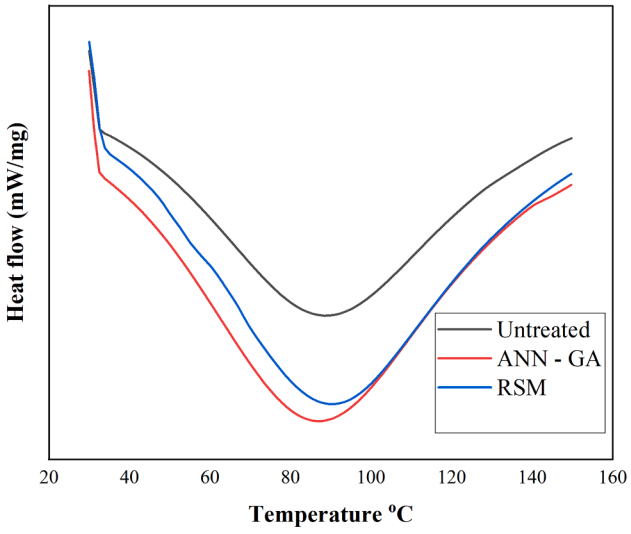

a)

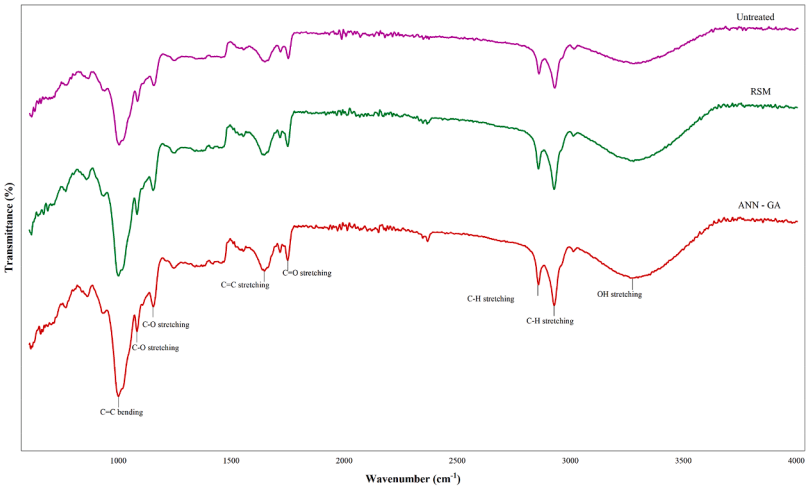

b)

Fig. 3. a) Thermographs of untreated, optimized RSM and ANN – GA of kodo millet flour b) Infrared spectra of untreated, optimized RSM and ANN – GA of kodo millet flour.

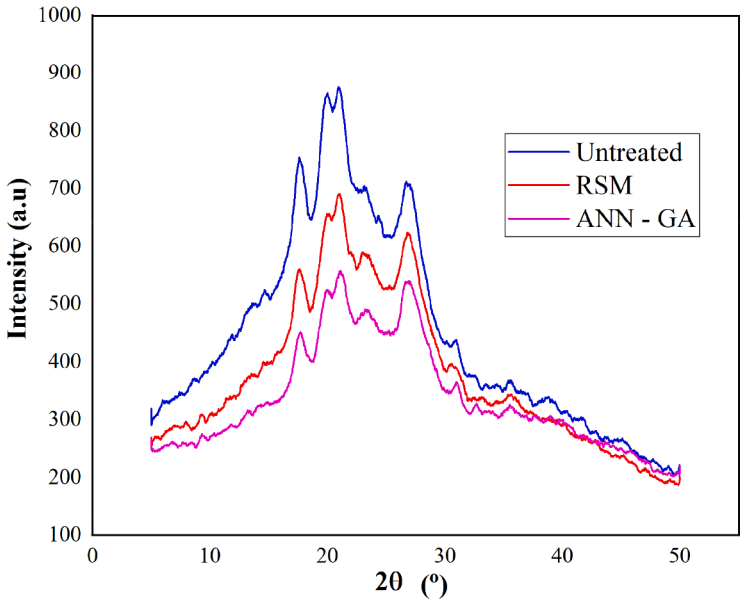

a)

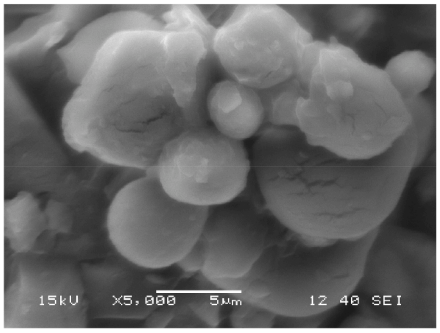

b) Untreated

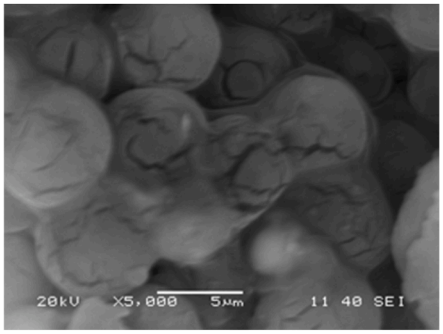

b) RSM

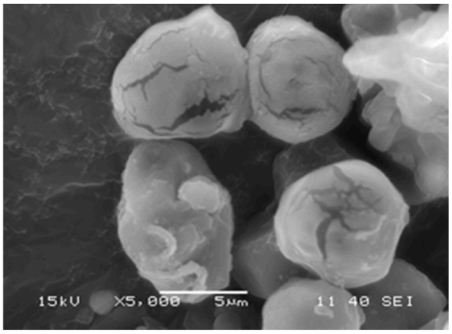

b) ANN – GA

Fig. 4. a) Diffractograms of untreated, optimized RSM and ANN – GA of kodo millet flour b) Micrographs of untreated, optimized RSM and ANN – GA of kodo millet flour.

model is far better than RSM model in predicting the responses (Jisha et al., 2008; Pradhan et al., 2021). Hence, ANN – GA model is much suitable for improving the functional properties of kodo millet flour.

3.4. *Thermographs of kodo millet flour*

The DSC graphs of untreated, optimized RSM and ANN – GA treated kodo millet flour were shown in Fig. 3 a). Both RSM and ANN – GA optimized conditions used for treated kodo millet flour resulted in decreased peak temperatures. The reduction in peak temperature might be due to starch granules depolymerization or variation in ratio of amylose and amylopectin by plasma reactive nitrogen and oxygen species. Similar results were reported that potato samples decreased the gelatinization of starch in potato when samples were treated with N_2 plasma 2 kPa for treatment times of 30, 45 and 60 min (Zhang, Chen, Li, Li, & Zhang, 2015).

3.5. Infra red spectra of kodo millet flour

IR spectra of untreated, optimized RSM and ANN – GA treated kodo millet flour and the peaks were observed at 995, 1075, 1147, 1640, and 1709 cm^{-1} corresponds to their groups were shown in Fig. 3 b). The peaks of both RSM and ANN – GA were revealed in increased absorption. The wide range of peak was at 3289 cm^{-1} obtained from ANN – GA and other bonds at 2852 and 2920 cm^{-1} and strong intermolecular bonds by reactive plasma species mainly RNS and ROS. These bonds are responsible for starch depolymerization of components. Similar absorption peaks were reported by other researchers (Zhou, Yan, Shi, & Liu, 2019; Chaple et al., 2020).

3.6. Diffractograms of kodo millet flour

X-ray diffractograms of untreated, optimized RSM and ANN – GA treated kodo millet flour were shown in Fig. 4 a). Negative correlation was reported in crystallinity with voltage and treatment time for both RSM and ANN – GA. Moreover ANN – GA had less crystallinity than RSM. Reduction in crystallinity was due to action of reactive active species of the plasma broke down the starch granules. Previous researchers were also reported similar results (Wongsagonsup et al., 2014; Zhang et al., 2015; Zhou et al., 2019; Sarangapani, Devi, Thirundas, Annapure, & Deshmukh, 2015).

3.7. Scanning electron microscopy analysis (SEM)

The images of untreated, optimized RSM and ANN – GA treated kodo millet flour particles were obtained from SEM shown in Fig. 4 b). Morphological structure of kodo millet flour particles (untreated and treated) was observed in microscope. The displayed micrographs of particles have basically round or spherical with smooth surface structure and most of these were undamaged in untreated flours whereas cracking of flour granule was very much visualised in both treated samples. It was clearly evident that rise in voltage and treatment time eventually causing broke down of granules. Reactive species obtained from plasma causes etching and proliferation into flour particle thus lead to depolymerisation of starch molecules and dissociation of cross linkages of starch molecules. Same was mentioned by researchers (Chen, 2014; Thirumdas, Saragapani, Ajinkya, Deshmukh, & Annapure, 2016; Lii, Liao, Stobinski, & Tomasik, 2002a, 2002b) that after the plasma treatment, fissures in starch granules were formed and reported.

4. Conclusion

The hydration properties of kodo millet flour after plasma treatment were analyzed. The analyzed values were predicted and optimized by RSM and ANN – GA. Optimized values of RSM at 20 kV voltage and 17.9 min for WAC, OAC, SI and SC were 1.5085 g/g, 1.4045 g/g, 0.0591 g/g and 3.6757 g/g, respectively. Whilst the ANN optimized values at 17.1 kV voltage and 23.3 min for WAC, OAC, SI and SC were 1.5129 g/g, 1.5002 g/g, 0.0616 g/g and 4.388 g/g respectively. Instrumental analysis like DSC, FTIR, SEM and XRD were also performed for both RSM and ANN optimized conditions, which revealed significant difference with untreated samples. RSM and ANN, both have shown good predictability. The obtained R^2 value was higher in ANN and remaining parameters MSE, RSME, NSME, NRSME, AAD, and MPE values were minimum. This resulted that ANN had superior model than RSM with good accuracy and better performance.

Declaration of Competing Interest

The authors declare that they have no known competing financial interests or personal relationships that could have appeared to influence the work reported in this paper.

Acknowledgments

Funding was provided for this research by the Science and Engineering Research Board (SERB), Core-Research Grant (File No.: CRG/2020/002551), Department of Science & Technology (DST), New Delhi, Government of India.

Appendix A. Supplementary data

Supplementary data to this article can be found online at https://doi.org/10.1016/j.fochms.2022.100132.

References

Abdullah, S., Pradhan, R. C., Aflah, M., & Mishra, S. (2020). Efficiency of tannase enzyme for degradation of tannin from cashew apple juice: Modeling and optimization of process using artificial neural network and response surface methodology. *Journal of Food Process Engineering, 43*, 1–10. https://doi.org/10.1111/jfpe.13499

Abdullah, S., Pradhan, R. C., Pradhan, D., & Mishra, S. (2021). Modeling and optimization of pectinase-assisted low-temperature extraction of cashew apple juice using artificial neural network coupled with genetic algorithm. *Food Chemistry, 339*, Article 127862. https://doi.org/10.1016/j.foodchem.2020.127862

Arya, S. S., & Shakya, N. K. (2021). High fiber, low glycaemic index (GI) prebiotic multigrain functional beverage from barnyard, foxtail and kodo millet. *LWT, 135*. https://doi.org/10.1016/j.lwt.2020.109991

Bie, P., Pu, H., Zhang, B., Su, J., Chen, L., & Li, X. (2016). Structural characteristics and rheological properties of plasma-treated starch. *Innovative Food Science and Emerging Technologies., 34*, 196–204. https://doi.org/10.1016/j.ifset.2015.11.019

Chaple, S., Sarangapani, C., Jones, J., Carey, E., Causeret, L., Genson, A., … Bourke, P. (2020). Effect of atmospheric cold plasma on the functional properties of whole wheat (Triticum aestivum L.) grain and wheat flour. *Innovative Food Science and Emerging Technologies., 66*, Article 102529. https://doi.org/10.1016/j.ifset.2020.102529

Chen, H. H. (2014). Investigation of properties of long-grain brown rice treated by low-pressure plasma. *Food and Bioprocess Technology, 7*, 2484–2491. https://doi.org/10.1007/s11947-013-1217-2

Cordelino, I. G., Tyl, C., Inamdar, L., Vickers, Z., Marti, A., & Ismail, B. P. (2019). Cooking quality, digestibility, and sensory properties of proso millet pasta as impacted by amylose content and prolamin profile. *Lwt, 99*, 1–7. https://doi.org/10.1016/j.lwt.2018.09.035

Ferguson, L. R. (2001). Role of plant polyphenols in genomic stability. *Mutation Research/Fundamental and Molecular Mechanisms, 475*, 89–111. https://doi.org/10.1016/S0027-5107(01)00073-2

Godswill, C., Somtochukwu, V., & Kate, C. (2019). The functional properties of foods and flours. *International Journal of Advanced Research, 5*, 2488–9849.

P.S. Hegde, G. Chandrakasan, T.S. Chandra, Inhibition of collagen glycation and crosslinking in vitro by methanolic extracts of Finger millet (Eleusine coracana) and Kodo millet (Paspalum scrobiculatum), 2002.

S. Jaddu, R.C. Pradhan, M. Dwivedi, Effect of multipin atmospheric cold plasma discharge on functional properties of little millet (Panicum miliare) flour, 77 (2022).

Jisha, S., Padmaja, G., Moorthy, S. N., & Rajeshkumar, K. (2008). Pre-treatment effect on the nutritional and functional properties of selected cassava-based composite flours. *Innovative Food Science and Emerging Technologies., 9*, 587–592. https://doi.org/10.1016/j.ifset.2008.06.003

Kusumayanti, H., Handayani, N. A., & Santosa, H. (2015). Swelling power and water solubility of cassava and sweet potatoes flour. *Procedia Environ. Sci., 23*, 164–167. https://doi.org/10.1016/j.proenv.2015.01.025

Lii, C. Y., Liao, C. D., Stobinski, L., & Tomasik, P. (2002a). Effects of hydrogen, oxygen, and ammonia low-pressure glow plasma on granular starches. *Carbohydrate Polymers, 49*, 449–456. https://doi.org/10.1016/S0144-8617(01)00351-4

Lii, C. Y., Liao, C. D., Stobinski, L., & Tomasik, P. (2002b). Behaviour of granular starches in low-pressure glow plasma. *Carbohydrate Polymers, 49*, 499–507. https://doi.org/10.1016/S0144-8617(01)00365-4

Nanje Gowda, N. A., Siliveru, K., Vara Prasad, P. V., Bhatt, Y., Netravati, B. P., & Gurikar, C. (2022). Modern processing of Indian millets: a perspective on changes in nutritional properties. *Foods, 11*, 1–18. https://doi.org/10.3390/foods11040499

Obadi, M., Zhu, K. X., Peng, W., Sulieman, A. A., Mohammed, K., & Zhou, H. M. (2018). Effects of ozone treatment on the physicochemical and functional properties of whole grain flour. *Journal of Cereal Science, 81*, 127–132. https://doi.org/10.1016/j.jcs.2018.04.008

Patra, A., Abdullah, S., & Pradhan, R. C. (2021). Application of artificial neural network-genetic algorithm and response surface methodology for optimization of ultrasound-assisted extraction of phenolic compounds from cashew apple bagasse. *Journal of Food Process Engineering, 44*. https://doi.org/10.1111/jfpe.13828

D. Pradhan, S. Abdullah, R.C. Pradhan, Optimization of pectinase assisted extraction of chironji (Buchanania Lanzan) fruit juice using response surface methodology and artificial neural network, International Journal of Fruit Science 20 (2020) S318–S336. 10.1080/15538362.2020.1734895.

[12] D. Pradhan, S. Abdullah, R.C. Pradhan, Chironji (Buchanania lanzan) fruit juice extraction using cellulase enzyme: modelling and optimization of process by artificial neural network and response surface methodology, Journal of Food Science and Technology 58 (2021) 1051–1060. 10.1007/s13197-020-04619-8.

Ramashia, S. E., Gwata, E. T., Meddows-Taylor, S., Anyasi, T. A., & Jideani, A. I. O. (2018). Some physical and functional properties of finger millet (Eleusine coracana) obtained in sub-Saharan Africa. *Food Research International, 104*, 110–118. https://doi.org/10.1016/j.foodres.2017.09.065

Rao, B., Nagasampige, M., & Ravikiran, M. (2011). Evaluation of nutraceutical properties of selected small millets. *Journal of Pharmacy and Bioallied Sciences., 3*, 277–279. https://doi.org/10.4103/0975-7406.80775

M.V. Rao, A. KG, S. CK, V. N, J. R, Effect of microwave treatment on physical and functional properties of foxtail millet flour, International Journal of Chemical Studies 9 (2021) 2762–2767. 10.22271/chemi.2021.v9.i1am.11641.

Sarangapani, C., Devi, Y., Thirundas, R., Annapure, U. S., & Deshmukh, R. R. (2015). Effect of low-pressure plasma on physico-chemical properties of parboiled rice. *Lwt., 63*, 452–460. https://doi.org/10.1016/j.lwt.2015.03.026

Sharma, S., Saxena, D. C., & Riar, C. S. (2016). Nutritional, sensory and in-vitro antioxidant characteristics of gluten free cookies prepared from flour blends of minor millets. *Journal of Cereal Science, 72*, 153–161. https://doi.org/10.1016/j.jcs.2016.10.012

Sharma, S., Sharma, N., Handa, S., & Pathania, S. (2017). Evaluation of health potential of nutritionally enriched Kodo millet (Eleusine coracana) grown in Himachal Pradesh, India. *Food Chemistry, 214*, 162–168. https://doi.org/10.1016/j.foodchem.2016.07.086

Sharma, S., Saxena, D. C., & Riar, C. S. (2017). Using combined optimization, GC–MS and analytical technique to analyze the germination effect on phenolics, dietary fibers, minerals and GABA contents of Kodo millet (Paspalum scrobiculatum). *Food Chemistry, 233*, 20–28. https://doi.org/10.1016/j.foodchem.2017.04.099

Sin, H. N., Yusof, S., Hamid, N. S. A., & Rahman, R. A. (2006). Optimization of enzymatic clarification of sapodilla juice using response surface methodology. *Journal of Food Engineering, 73*, 313–319. https://doi.org/10.1016/j.jfoodeng.2005.01.031

Thirumdas, R., Saragapani, C., Ajinkya, M. T., Deshmukh, R. R., & Annapure, U. S. (2016). Influence of low pressure cold plasma on cooking and textural properties of brown rice. *Innovative Food Science and Emerging Technologies, 37*, 53–60. https://doi.org/10.1016/j.ifset.2016.08.009

Wongsagonsup, R., Deeyai, P., Chaiwat, W., Horrungsiwat, S., Leejariensuk, K., Suphantharika, M., … Dangtip, S. (2014). Modification of tapioca starch by non-chemical route using jet atmospheric argon plasma. *Carbohydrate Polymers, 102*, 790–798. https://doi.org/10.1016/j.carbpol.2013.10.089

Zhang, B., Chen, L., Li, X., Li, L., & Zhang, H. (2015). Understanding the multi-scale structure and functional properties of starch modulated by glow-plasma: A structure-functionality relationship. *Food Hydrocolloids, 50*, 228–236. https://doi.org/10.1016/j.foodhyd.2015.05.002

Zhou, Y., Yan, Y., Shi, M., & Liu, Y. (2019). Effect of an atmospheric pressure plasma jet on the structure and physicochemical properties ofwaxy and normal maize starch. *Polymers (Basel)., 11*. https://doi.org/10.3390/polym11010008